THE INVERSE-DEFORMATION APPROACH TO FRACTURE

Phoebus Rosakis, Timothy J. Healey and Ugur Alyanak

1. Introduction

Most current brittle-fracture models introduce the crack as a separate entity, a priori endowed with properties that are distinct from the constitutive law of the bulk material. In addition, the fact that fracture involves discontinuous deformations is problematic, because such deformations cannot be approximated by smooth functions and still maintain bounded elastic energy, especially if higher-gradients are included in the model. An attempt to circumvent such problems was Truskinovsky's Fracture as a Phase Transition [?]. In this approach, fracture results from nonconvexity of the stored energy function, but it involves strains in the fracture zone that become unbounded as the transformation strain goes to infinity. It would be desirable to regularize the problem using higher gradients, but this leads to infinite energies in the same limit. Indeed, any approximation of a cracked deformation by smooth ones would have unbounded higher gradient energy in the limit.

Here we develop a nonlinear elastic, local constitutive model that can predict fracture automatically as a phase transition via a standard bifurcation analysis, is amenable to regularization by higher gradients, and does not involve discontinuous deformations, additional field variables, such as damage or phase-field variables, or a separately specified surface energy.

Our first observation concerns one-dimensional fractured deformations, viewed here as strictly monotone mappings that involve at least one jump discontinuity. The graph of such a function has disjoint pieces, that can be joined together by vertical segments of "infinite slope" (see Fig. 1a). One can then easily construct a generalized inverse of this deformation, by interchanging the abscissa and the ordinate. The graph of this inverse has strictly increasing pieces that are the graphs of the (standard) inverses of the deformation on either side of the crack. Moreover their graphs are connected by a horizontal segment, which corresponds to the "inverse" of the segment of infinite slope. The generalized inverse so constructed is a piecewise smooth mapping, where two or more "phases" of positive stretch are separated by one or more intervals of zero stretch. One would then extend the notion of deformation to admit nonnegative, as opposed to strictly positive, derivatives, so that mere (non strict) monotonicity is required.

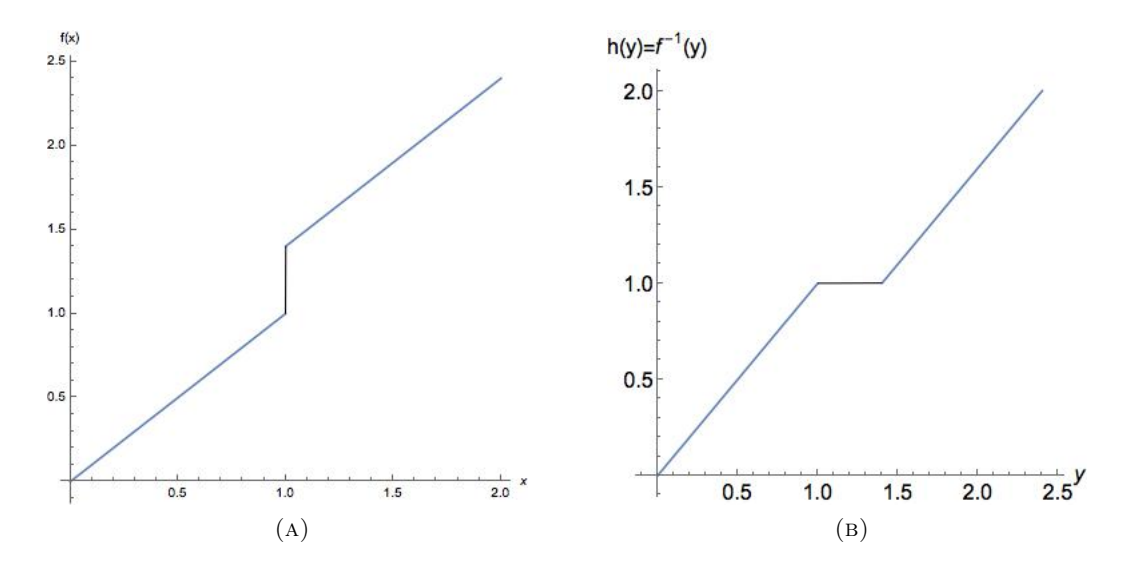


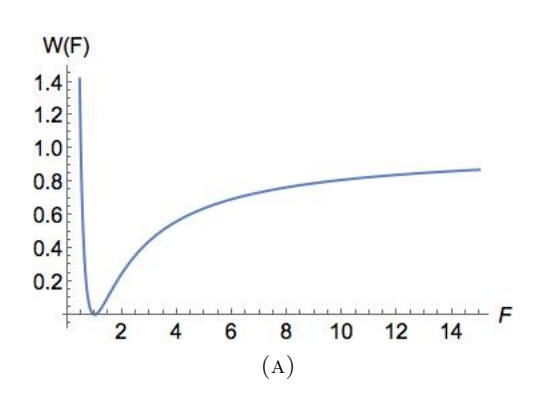
FIGURE 1. (A) A cracked deformation (blue) with a vertical segment (black) attached to render the graph a continuous curve. (B) The generalized inverse of the cracked deformation. The horizontal segment (black) is the opened crack in the deformed configuration.

In a sense, the inverse deformation closes the crack, as it maps each crack interval to a single point, the reference location of the crack. Analogously, the original deformation opens the crack, as it maps the single crack point in the reference configuration to the cracked interval in the deformed one.

A major advantage is that unlike the discontinuous original deformation, the generalized inverse, Fig. 1b, is Lipschitz continuous and has mere gradient discontinuities, like a two-phase deformation [?]. Here intervals of positive stretch are separated by intervals of zero stretch. These we identify with the uncracked phase and the cracked phase, respectively. The length of a cracked-phase interval is nothing but the crack opening displacement.

Another crucial advantage of the inverse description is that the analogy with phase transitions extends naturally to the constitutive law itself, once we invoke the inverse deformation approach of Shield [?], as we now explain. Typically, in one dimension, a material that suffers brittle fracture would have an elastic stored energy function of the form shown in Fig. 2b, having a convex well at the reference state, but eventually becoming concave and approaching a horizontal asymptote from below as the stretch tends to infinity. The inverse stored energy function W is related to the (usual) stored energy function W by [?]?

$$W(H) = HW(1/H), \quad H > 0$$



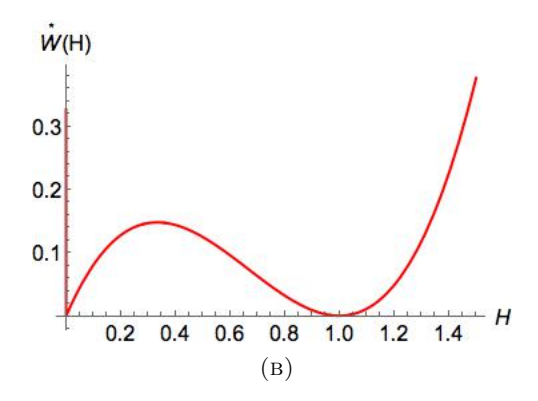


FIGURE 2. (A) A stored energy function of a material that undergoes brittle fracture. (B) The corresponding inverse stored energy function.

and has the property that the elastic energy of a deformation $f:[0,1] \to [0,\lambda]$ can be written as

$$\int_0^1 W(f'(x))dx = \int_0^\lambda \overset{*}{W}(h'(y))dy$$

where $h=f^{-1}$ is the inverse deformation. For W as in Fig. 2a, the inverse stored energy $\stackrel{*}{W}$ would be as in Fig. 2b,, where we now extend its domain of definition as follows

$$\overset{*}{W}(H) = \begin{cases} HW(1/H), & H > 0 \\ 0, & H = 0 \\ \infty, & H < 0. \end{cases}$$

Here we allow the possibility that the inverse stretch H := h' = 0 (corresponding to the cracked phase as discussed above) but prohibit h' < 0, which corresponds to f' < 0, that is, orientation-reversing interpenetration. We recall that the case h' = 0 corresponds to crack opening, not interpenetration. Instead of the usual constraint f' > 0 we thus impose $h' \ge 0$ as a constraint. When one visualizes this unilateral constraint as a vertical barrier at 0 as part of the graph of W (Fig. 2b), it is clear that the latter has the form of a two-well energy, with wells at 0 and 1, while the inverse deformation of Fig. 1b is a zero-energy one (global minimizer) provided the slopes of the rising portions equal 1. In Fig. 2b, the well at 1 corresponds to the undeformed, uncracked state, while the one at 0 to the cracked state. The length of the part in the 0 phase in Fig. 2b (horizontal segment) is the crack opening displacement. In this sense, the 0 phase is "thin air" or empty space between crack faces.

A standard minimization of this two-well energy gives the convexification \widehat{W} of \widehat{W} (together with the constraint $h' \geq 0$). This corresponds to a material that cannot resist compression (Fig. 3a). Also \widehat{W} is the inverse stored energy function of \widehat{W} , which has the form shown in Fig. 3b, corresponding to a material that cannot sustain tension. The drawback here is that minimizers h of the inverse energy can have an arbitrary number of

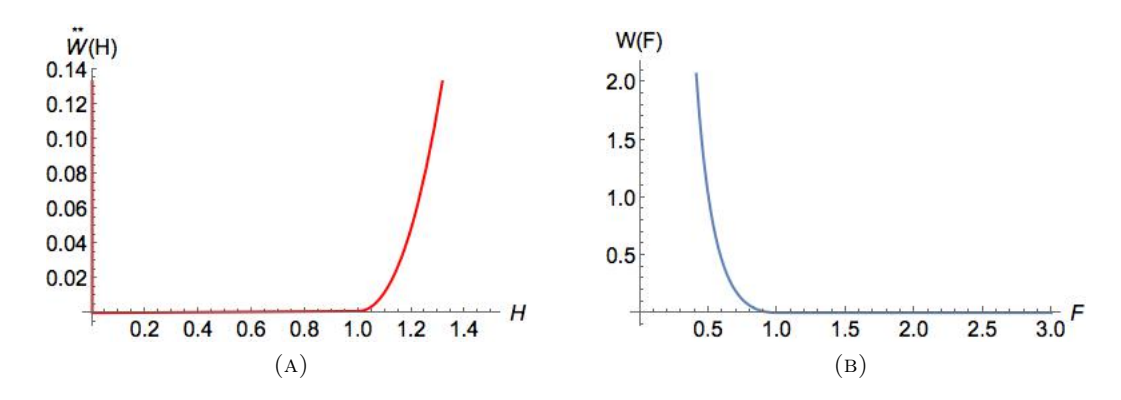


FIGURE 3. (A) The convexification $\overset{**}{W}$ of $\overset{*}{W}$ of Fig. 2b. (B) The stored energy function \hat{W} whose inverse stored energy is $\overset{**}{W}$.

cracked intervals h' = 0 alternating with intervals where h' = 1, corresponding to arbitrary positions of cracks in the reference configuration.

The final advantage of the inverse approach is that the problem associated with W can be regularized by the addition of higher gradients of the inverse deformation h to the energy which would become

$$E_{\varepsilon}\{h\} = \int_0^{\lambda} W(h'(y))dy + \frac{\varepsilon^2}{2} \int_0^{\lambda} [h''(y)]^2 dy$$
 (1.1)

The analogous attempt to add higher gradients of the original deformation f to the energy runs into difficulties because of the discontinuities of f (Fig. 1a).

We study equilibria of the displacement problem in the inverse formulation. While we could employ global energy minimisation of (1.1), we choose instead to follow the path of global bifurcation (no pun intended), keeping in mind that stable branches of local energy minima may occur, while exploiting phase plane techniques in the spirit of [?]. The only complication here is the unilateral constraint $h' \geq 0$ on the inverse deformation in an otherwise fairly standard two-well problem with higher gradients like [?, ?].

A physical description of the results is what one expects from a fracture model worth its salt, and agrees with predictions of discrete models [?]: In particular, pulling on a bar eventually breaks it at one of the two ends and the stress vanishes thereafter. The broken end has an additional surface energy (because of higher gradients) as posited by Griffith. Solutions with more fractures than one are unstable. Longer bars are more brittle (break sooner and more suddenly) than shorter bars.

The strength of the inverse approach lies in the simplicity of model (1.1) and the mathematical ease with which these conclusions are reached. This is promising, and it begs the question of two or three dimensional formulations, which we pursue elsewhere [].

The outline of this paper is as follows:

```
OUTLINE
SURFACE ENERGY (Griffith)
SCALE EFFECT
STABILITY
HIGHER dimension
```

Our assumptions for $W(\text{and thus for } W^*)$ are in accordance with the properties suggested in Figure 2:

```
W \in C^3(0,\infty); \ W(F) \nearrow \infty \text{ as } F \searrow 0; \ W(F) \nearrow \gamma > 0 \text{ as } F \nearrow \infty; W(1) = 0; \ W > 0, \ F \neq 1; W is strictly convex on [0,1/\kappa) and strictly concave on (1/\kappa,\infty), where 0 < \kappa < 1. (1.2)
```

As a consequence of (1.2), it follows that

$$W^* \in C^3(0,\infty); \ W^*(0) = W^*(1) = 0; \ W^* > 0, \ H \neq 1; \ \dot{W}^*(0^+) := W_H^*(0^+) = \gamma;$$

 W^* is strictly concave on $[0,\kappa)$ and strictly convex on (κ,∞) .

We now give an outline of the work. In Section 2 we consider the inverse-strain formulation, based on (1.3), presuming hard loading in the presence of the unilateral constraint, cf. (1.1). We then proceed with a change of variables rendering the problem amenable to a bifurcation analysis. We show that the linearized problem about the homogeneous solution admits a countable infinity of potential bifurcation points. In Section 3 we show that each of these are indeed bifurcation points, viz., we prove that each point found in Section 2 gives rise to a local "pitchfork" bifurcation. In Section 4 we show that the trivial homogeneous solution is locally stable (the potential energy is rendered a local minimum) up to the first bifurcation point, after which there is an exchange of stability. We then infer that all local "higher-mode" branches, emanating for the second and higher bifurcation points are unstable.

In Section 5 we demonstrate that each local bifurcation path is, in fact, a subset of a global continuum of solutions, subject to the Rabinowitz alternatives [R]. In Section 6 we obtain a priori bounds on all nontrivial solutions. In Section 7, we use a well-known argument to show that the global bifurcating branches are separated from each other by virtue of the nodal properties of their respective solutions, and we eliminate one of the alternatives of the Rabinowitz theorem, cf. [CR] In addition, we demonstrate that each of the global bifurcating branches is bounded and terminates in fracture. Finally, Section 7 closes with an argument from [CGS], demonstrating that all solutions on the global, higher-mode branches are unstable. Consequently, we focus on the first global bifurcating branch of solutions in Section 8. As in [LR], we present the global bifurcation diagram as an effective stress-strain diagram in terms of the original Lagrangian variables. We show that the generalized stress vanishes at the termination of the branch, and that the fracture always occurs at one of the ends of the bar. The projection of the first global branch connects the bifurcation point on the homogeneous stress-strain curve to the zero-stress line at a finite value of the hard-loading parameter, whereas the homogeneous stress-strain curve predicts fracture asymptotically at infinity. ...

2. Formulation

We begin with the total potential energy (1.2), written in terms of the inverse strain H = h':

$$E_{\varepsilon}[H] = \int_0^{\lambda} \left[\frac{\varepsilon}{2} (H')^2 + W^*(H) \right] dy, \tag{2.1}$$

where $\lambda > 0$. We treat $\varepsilon > 0$ as a fixed small parameter throughout. We consider "hard" loading, viz., h(0) = 0, $h(\lambda) = 1$; in terms of the inverse strain, this becomes

$$\int_0^{\lambda} H(y)dy = 1,$$

 $H \geqslant 0 \text{ on } [0, \lambda],$
(2.2)

for $\lambda \in \mathbb{R}^+ := (0, \infty)$,cf. (1.1). For convenience of our forthcoming analysis, we change variables as follows:

$$y = \lambda s, \quad 0 \le s \le 1,$$

$$u(s) := \lambda H(\lambda s) - 1.$$
 (2.3)

Then (2.1), (2.2) are equivalent to

$$V_{\varepsilon}[\lambda, u] = \int_{0}^{1} \left[\frac{\varepsilon}{2} (u')^{2} + \lambda^{4} \Gamma(\lambda, u) \right] ds, \tag{2.4}$$

subject to

$$\int_0^1 u ds = 0,
 u \ge -1 \text{ on } [0, 1],$$
(2.5)

respectively, where

$$\Gamma(\lambda, u) := W^*([1+u]/\lambda). \tag{2.6}$$

Next, we formally look for equilibria as critical points of $u \mapsto V_{\varepsilon}$ yielding the Euler-Lagrange equation

$$-\varepsilon u'' + \lambda^3 \rho(\lambda, u) - \mu = 0, \ 0 < x < 1, \tag{2.7}$$

subject to (2.5) and (2.7)

$$u'(0) = u'(1) = 0,$$

where

$$\rho(\lambda, u) := \dot{W}^* ([1 + u]/\lambda); \ \dot{W}^* := \frac{dW^*}{dH}.$$
 (2.8)

The natural boundary conditions $(2.7)_2$ imply that the Lagrange multiplier appearing in $(2.7)_1$ evaluates to

$$\mu = \lambda^3 \int_0^1 \rho(\lambda, u(\tau)) d\tau. \tag{2.9}$$

We observe that $u \equiv 0$ is a solution of (2.7)-(2.9) for all $\lambda \in \mathbb{R}^+ := (0, \infty)$, and we look for bifurcation from this trivial solution ray. Accordingly, we investigate the formal linearization at u = 0:

$$-\varepsilon u'' + \lambda^2 \ddot{W}^*(1/\lambda)u = 0, \quad 0 < x < 1,$$

$$u'(0) = u'(1) = 0, \quad \int_0^1 u ds = 0,$$
 (2.10)

where $\ddot{W}^* := \frac{d^2W^*}{dH^2}$. Clearly (2.10) admits nontrivial solutions

$$u = \phi_n := \cos(n\pi s), \quad n = 1, 2, ...,$$
 (2.11)

provided that the characteristic equation

$$\frac{\varepsilon n^2 \pi^2}{\lambda^2} = -\ddot{W}^*(1/\lambda),\tag{2.12}$$

has corresponding "roots" λ_n , n=1,2,... For each value of $n \in \mathbb{N}$, the left side of (2.11) defines a parabola in the variable " $1/\lambda$ ". Then taking into account the graph of $-\ddot{W}^*(\cdot)$, cf. (1.2) and Figure 4, we conclude that (2.12) has a countable infinity of simple (transversal) roots:

$$1/\kappa < \lambda_1 < \lambda_2 < \dots, \tag{2.13}$$

each of which corresponds to a respective nontrivial solution (2.11).

3. Local Bifurcation

In order to carry out a rigorous bifurcation analysis, we introduce operator notation on appropriate function spaces as follows:

$$X^{k} := \{ v \in C^{k}(\mathbb{R}) : v(s) \equiv v(s+2) \equiv v(-s), \int_{0}^{1} v ds = 0 \}, \quad k = 0, 1, 2.$$
 (3.1)

We let $\|v\|_k$ denote the usual maximum norm on [0,1], i.e., $\|v\|_0 = \max_{s \in [0,1]} |v(s)|$, $\|v\|_1 = \|v\|_0 + \|v'\|_0$, etc.; each of (3.1) so equipped is a Banach space. We then view (2.7)₁ to be defined for all $x \in \mathbb{R}$, and identify it with a mapping $F : \mathbb{R}^+ \times (\mathcal{O} \subset X^2) \to X^0$, where

$$\mathcal{O} := \{ u \in X^2 : u > -1 \text{ on } [0, 1] \}. \tag{3.2}$$

Observe that any solution of

$$F(\lambda, u) = 0, (3.3)$$

satisfies (2.5) and the boundary conditions $(2.7)_2$. A routine phase-plane analysis of (2.7) (cf. Section 6) shows that the converse holds, viz., any solution of (2.7) fulfilling $(2.5)_1$ and $(2.5)_2$ strictly, is also a solution of (3.3).

We note that $F(\lambda,0)=0$ for all $\lambda\in(0,\infty)$, and our previous formal calculations (2.10)-(2.13) are rigorous consequences of the fact that $F(\cdot)$ is a C^1 mapping: Let $A(\lambda):=D_uF(\lambda,0):X^2\to X^0$, denote the Frechet derivative of $u\mapsto F(\lambda,u)$ at u=0. Then (2.10) is equivalent to

$$A(\lambda)u = 0, (3.4)$$

and (2.11)-(2.13) imply

$$A(\lambda_n)\phi_n = 0, \quad n \in \mathbb{N},\tag{3.5}$$

which constitutes a necessary condition for bifurcation at $(\lambda_n, 0)$, n = 1, 2, ... It's easy to show that the inhomogeneous equation

$$A(\lambda)u = b, (3.6)$$

has a unique solution $u \in X^2$, for all $b \in X^0$, provided that $\lambda \neq \lambda_n$, n = 1, 2, ..., cf. (2.13). On the other hand, for each values of $\lambda = \lambda_n$ given by (2.13), standard ODE methods for constant-coefficient 2^{nd} -order equations show that (3.6) admits the homogeneous solution (2.11) times an arbitrary constant plus a particular solution, the latter of which exists provided that $\int_0^1 \phi_n b ds = 0$. We conclude that $A(\lambda) \in L(X^2, X^0)$ is a Fredholm operator of index zero, i.e., the dimension of the null space agrees with the co-dimension of the range.

As a consequence, we may employ the well-known Liapunov-Schmidt method to investigate simple bifurcation in the neighborhood of the points $(\lambda_n, 0), n = 1, 2, ..., cf.$ [CR], [K]. In particular, it's enough to verify the "crossing condition"

$$A'(\lambda_n)\phi_n \notin \text{Range}(A(\lambda_n)).$$
 (3.7)

From (2.10) and (3.4), we find $A'(\lambda_n)\phi_n = C_n\phi_n$, where $C_n := 2\lambda_n \ddot{W}^*(1/\lambda_n) - (\lambda_n)^2 \ddot{W}^*(1/\lambda_n) < 0, n = 1, 2, ..., \text{cf. } (1.2), (2.13).$ Moreover, from (2.10) it follows that $A(\lambda_n)$ is formally self-adjoint, and

$$\int_0^1 (A'(\lambda_n)\phi_n)\phi_n dx = C_n \int_0^1 \cos^2 n\pi x dx \neq 0,$$
(3.8)

which verifies (3.7). We now have:

Proposition 3.1 For each n = 1, 2, ..., there is an open neighborhood of $(0, \lambda_n)$, denoted $\mathcal{N}_n \subset \mathbb{R}^+ \times \mathcal{O}$, and a unique local path of non-trivial solutions of (2.3) given by

$$\mathcal{P}_n := \{ (\lambda, u) = (\tilde{\lambda}_n(t), t(\phi_n + \psi_n(t)) : t \in J \} \subset \mathcal{N}_n, \tag{3.9}$$

where $\tilde{\lambda}_n: J \to \mathbb{R}$ and $\psi_n: J \to X^2$ are each continuously differentiable on some open interval J containing 0, with $\tilde{\lambda}_n(0) = \lambda_n$ and $\psi_n(0) = 0$. Moreover, $\tilde{\lambda}'_n(0) = 0$, i.e., each \mathcal{P}_n represents a "pitchfork".

Remark 3.2 The very last part above follows from the observation that $F(\lambda, \sigma u) = \sigma F(\lambda, u)$, where $\sigma u(s) := u(s-1)$, which is the forward shift by one-half the period, cf. [GS I], [HP].

4. Stability of Local Solutions

In this section we adopt the usual energy criterion for stability, viz., an equilibrium solution is locally stable—if it renders the potential energy a local minimum; if not, the equilibrium is unstable. Referring to (2.4), we note that $V_{\varepsilon}: \mathbb{R}^+ \times X^1 \to \mathbb{R}$ is a C^2 functional. Thus, we may rigorously employ the second-derivative test (second variation) to obtain weak local minima. We first consider the trivial solution.

Proposition 4.1 The trivial solution $u \equiv 0$ is stable for all $\lambda \in (0, \lambda_1)$ and unstable for all $\lambda \in (\lambda_1, \infty)$, where $(\lambda_1, 0) \in \mathbb{R}^+ \times X^2$ is the first bifurcation point, cf. (2.13) and Proposition 2.1.

Proof. The second variation of (2.4) at $u \equiv 0$ is given by

$$\delta^2 V_{\varepsilon}[\lambda, 0; \eta] := \frac{d^2}{d\tau^2} V_{\varepsilon}[\lambda, \tau \eta]|_{\tau=0} = \int_0^1 \left[\varepsilon(\eta')^2 + \lambda^2 \ddot{W}^*(1/\lambda) \eta^2 \right] ds, \tag{4.1}$$

for all variations $\eta \in X^1$. The Lagrange multiplier does not appear above, due to the fact that the constraint $(2.5)_1$ is linear, cf. [Z]. Next we employ the sharp Poincaré inequality

$$\int_0^1 (\eta')^2 ds \geqslant \pi^2 \int_0^1 \eta^2 ds,\tag{4.2}$$

where π^2 is the first eigenvalue of the operator $-\eta''$ on X^2 . Then (4.1), (4.2) lead to

$$\delta^{2}V_{\varepsilon}[\lambda, 0; \eta] \geqslant \left[\varepsilon \pi^{2} + \lambda^{2} \ddot{W}^{*}(1/\lambda)\right] \int_{0}^{1} \eta^{2} ds. \tag{4.3}$$

In view of (2.12) with n=1, and from the graph of $-\ddot{W}^*(\cdot)$, we conclude that $\varepsilon \pi^2/\lambda^2 > -\ddot{W}^*(1/\lambda)$ for all $1/\lambda > 1/\lambda_1$, cf. (1.2) and Figure 4. Of course this implies that (4.3) is positive for all $\lambda \in (0, \lambda_1)$ and $\eta \in X^1$.

For any $\lambda > \lambda_k$, choose the admissible test functions $\eta_\ell := \cos(\ell \pi s)$, for $\ell = 1, 2, ..., k$. Then

$$\delta^2 V_{\varepsilon}[\lambda, 0; \eta_{\ell}] = [\varepsilon \ell^2 \pi^2 + \lambda^2 \ddot{W}^*(1/\lambda)]/2. \tag{4.4}$$

Again, from (2.12) and the graph of $\ddot{W}^*(\cdot)$, we see that $\varepsilon \ell^2 \pi^2 / \lambda^2 < -\ddot{W}^*(1/\lambda)$, implying that $\delta^2 V_{\varepsilon}[\lambda, 0; \eta_{\ell}] < 0$, for $\ell = 1, 2, ..., k$. \square

Since each $(0, \lambda_n), n = 1, 2, ...$, is a simple bifurcation point, the results of Proposition 4.1 and well-known exchange-of-stability arguments give immediate information concerning the stability of the local pitchfork bifurcating solutions given by Proposition 3.1. If $(\lambda, u) \in \mathcal{P}_1$, then u will be stable or unstable if the pitchfork is supercritical or subcritical, i.e., if $\tilde{\lambda}'_1(0) > 0$ or $\tilde{\lambda}'_1(0) < 0$, respectively, cf. [K]. Assuming sufficient smoothness of W^* , a formula from [K] gives

$$\tilde{\lambda}_1'(0) = 3\ddot{W}^*(1/\lambda_1)/8,$$

which can be positive or negative, depending on the sign of $\widetilde{W}^*(1/\lambda_1)$,i.e., the first local path can be stable or unstable. On the other hand, the other local solution paths \mathcal{P}_n , n = 2, 3, ..., are all unstable – regardless of the sign of $\widetilde{W}^*(1/\lambda_n)$. This is due to the fact that the second variation (4.4) is negative in two or more "directions" for all $\lambda > \lambda_1$. whereas the exchange of stability at a simple, supercritical pitchfork only involves one eigenvalue regaining positivity. We now summarize.

Proposition 4.2 If $(\lambda, u) \in \mathcal{P}_1$, then u is stable (unstable) if $W^*(1/\lambda_1) > 0$ (< 0). In the latter case (instability), the linear operator $D_uF(\lambda, u): X^2 \to X^0$ has one negative eigenvalue. If $(\lambda, u) \in \mathcal{P}_k$, k = 2, 3, ..., then u is unstable, and $D_uF(\lambda, u)$ has k - 1 negative eigenvalues if the pitchfork \mathcal{P}_k is supercritical, and k negative eigenvalues in the subcritical case.

5. Global Bifurcation

In order to obtain global results, we first consider the linear operator $L[v] := -\varepsilon v''$. Since zero is not an eigenvalue of $L: X^2 \to X^0$, the operator is bijective with a compact inverse $L^{-1}: X^0 \to X^0$. Clearly $L^{-1}: X^1 \to X^1$ is also compact. Now consider the operator equation

$$G(\lambda, u) := \varepsilon u - K(\lambda, u) = 0, \tag{5.1}$$

where

$$K(\lambda, u) := \lambda^3 L^{-1} \left[\rho(\lambda, u) - \int_0^1 \rho(\lambda, u(\tau) d\tau) \right], \tag{5.2}$$

 $K: \mathbb{R}^+ \times (\mathcal{A} \subset X^1) \to X^1$ is compact,

$$\mathcal{A} := \{ u \in X^1 : u > -1 \text{ on } [0, 1] \}, \tag{5.3}$$

and $G: \mathbb{R}^+ \times (\mathcal{A} \subset X^1) \to X^1$ is C^1 . Then any solution of (5.1) is a solution of (3.3), and vice-versa. In particular, each of the local, nontrivial solution paths (3.9) satisfy (5.1) as well.

The advantage of (5.1) is that the Leray-Schauder degree of $u \mapsto G(\lambda, u)$ is well defined, which we now exploit. The Frèchet derivative of $u \mapsto G$ at $(\lambda, 0)$ is given by

$$D_u G(\lambda, 0) = L^{-1} A(\lambda) = \varepsilon I - \lambda^2 \ddot{W}^* (1/\lambda) L^{-1} \in L(X^1), \tag{5.4}$$

cf. (2.10), (3.4). Hence, zero is a simple eigenvalue of $L^{-1}A(\lambda_n)$, with null space spanned by ϕ_n , for each root λ_n , n = 1, 2, ..., of (2.12), respectively, cf. (2.11), (2.13). Since L^{-1} is compact, $L^{-1}A(\lambda) = \varepsilon I - \lambda^2 \ddot{W}^*(1/\lambda)L^{-1}$ has Fredholm index zero for all $\lambda \in \mathbb{R}^+$. Finally, it's not hard to see from (3.7), (3.8) that the Leray-Schauder index of $\lambda \mapsto D_u G(\lambda, 0) =$ $L^{-1}A(\lambda)$ (along the trivial solution) changes sign at each root λ_n , n = 1, 2, ... Hence, the global bifurcation theorem of Rabinowitz is applicable to (5.1).

Theorem 5.1 For each $root\lambda_n$, n = 1, 2, ..., of (2.12), $(\lambda_n, 0)$ is a point of global bifurcation. That is, let S denote the closure of the set of all nontrivial $(u \neq 0)$ solution pairs of (5.1), and let C_n denote the component of S containing $(\lambda_n, 0)$. Then at least one of the following is true:

- $(i)C_n$ is unbounded in $\mathbb{R} \times X^1$;
- (ii) $C_n contains (\lambda_*, 0)$, with $\lambda_* \neq \lambda_n$;
- (iii) $C_n \not\subset \mathbb{R}^+ \times \mathcal{A}$.

6. A priori Bounds

We obtain bounds on nontrivial solutions $u \neq 0$ in this section. We only require upper bounds, given that $u \geqslant -1$ is automatic, cf. $(2.5)_2$. Recall that any nontrivial solution pair (λ, u) of (5.1) delivers a solution of (3.3). If $u \neq 0$, then by virtue of evenness and periodicity, it attains both its maximum and its minimum somewhere on the closed interval, i.e., there are points $s_m, s_M \in [0, 1]$ such that:

$$\max_{s \in [0,1]} u(s) = u(s_M), \quad \min_{s \in [0,1]} u(s) = u(s_m),
\text{with } u(s_m) < 0 < u(s_M),
u''(s_m) \ge 0 \text{ and } u''(s_M) \le 0,$$
(6.1)

where $(5.1)_2$ is a consequence of $(2.5)_1$. We now evaluate $(2.7)_1$ at s_m and at s_M , subtract the resulting equations and employ (2.8), $(6.1)_3$ to deduce

$$\dot{W}^*([1 + u(s_M)]/\lambda) \leqslant \dot{W}^*([1 + u(s_m)]/\lambda). \tag{6.2}$$

From the graph of \dot{W}^* , it follows that both $(6.1)_2$ and (6.2) can be fulfilled only if

$$0 < 1/\lambda \le M \text{ and } 0 \le [1 + u(s_m)]/\lambda < [1 + u(s_M)]/\lambda \le M,$$
 (6.3)

where M > 0 satisfies $\dot{W}^*(M) = \gamma$, cf. Figure 3. Of course (6.3) is equivalent to

$$\lambda \geqslant 1/M \text{ and } -1 \leqslant u(s_m) < u(s_M) \leqslant \lambda M - 1.$$
 (6.4)

Then $(2.3)_3$, (6.3) and (6.4) immediately yield:

Theorem 6.1. Any nontrivial solution pair (λ, u) , $u \neq 0$, of (5.1) satisfies

$$||u||_0 \leqslant C_\lambda := \max\{1, \lambda M - 1\};$$
 (6.5)

in terms of the inverse deformation $H(y) = [u(y/\lambda) + 1]/\lambda$, this becomes

$$\max_{y \in [0,\lambda]} |H(y)| \leqslant M. \tag{6.6}$$

Finally, there is a constant $C_{\lambda,\varepsilon}$, depending on λ and ε , but independent of u, such that

$$||u||_1 \leqslant C_{\lambda,\varepsilon}. \tag{6.7}$$

Proof. The estimate (6.7) is a direct consequences of (6.5) and (2.7)₁, (2.9). \Box

In view of (6.4), we have $\lambda \ge 1/M$ for any nontrivial solution pair. Accordingly we may refine Theorem 5.1 as follows:

Corollary 6.2 Alternatives (i), (iii) of Theorem 5.1 may be replaced by $(i)'C_n \subset \mathbb{R}^+ \times X^1$ is unbounded,

(iii) $C_n \cap \mathbb{R}^+ \times \partial \mathcal{A} \neq \emptyset$, i.e., there is $(\lambda, u) \in C_n$ with $\lambda \in \mathbb{R}^+$ and $u(s_o) = -1$ for some $s_o \in [0, 1]$,

respectively.

7. Detailed Properties of Global Bifurcating Solutions

We first observe that the global solution branches, $C_n, n = 1, 2, ...$, of Theorem 5.1 are mutually separated by nodal properties via a well-known argument [CR2]. Let \mathcal{Z}_{ℓ} denote the open set of all functions $v \in X^1$ having precisely ℓ zeros in (0,1),each of which is simple, with $v(0) \neq 0$ and $v(1) \neq 0$. Then by virtue of (2.11) and (3.9), it follows that each local path of non-trivial solutions satisfies

$$\mathcal{P}_n \setminus \{(\lambda_n, 0)\} \subset \mathbb{R}^+ \times \mathcal{Z}_n, n = 1, 2, ..., \tag{7.1}$$

for |J| sufficiently small. In fact, this property is inherited globally:

Proposition 7.1. Each of the global bifurcating branches of Theorem 5.1, C_n , n = 1, 2, ..., is characterized by distinct nodal properties, viz.,

$$C_n \setminus \{(\lambda_n, 0)\} \subset (\mathbb{R}^+ \times \mathcal{Z}_n), n = 1, 2, \dots$$
 (7.2)

As such, $C_n \cap C_m = \emptyset$, for all $m \neq n$, and each C_n , n = 1, 2, ..., is characterized by either alternative (i)' or alternative (iii)' of Corollary 6.2.

Proof. The argument given in [CR], [R] shows that nodal properties of solutions on global branches of 2^{nd} -order ODE, such as $(2.7)_1$, (2.9), can change only at the trivial solution. Given that C_n is a continuum, this relies on (7.1) and the uniqueness theorem.

Since $\mathcal{P}_n \subset \mathcal{C}_n$, the observation that $\mathcal{Z}_m \cap \mathcal{Z}_n = \emptyset$ for all $m \neq n$, then implies (7.2). This rules out alternative (ii) of Theorem 5.1 as well. \square

Next we find it convenient to return to the original variables via (2.3), in which case the equilibrium equation $(2.7)_1$ now reads

$$-\varepsilon H'' + \dot{W}^*(H) = \varpi, \tag{7.3}$$

where $\varpi = \mu/\lambda^3$. This along with (2.3), (2.8) and (2.9), yields

$$\varpi = \frac{1}{\lambda} \int_0^\lambda \dot{W}^*(H(t))dt. \tag{7.4}$$

The boundary conditions $(2.7)_2$ now become

$$H'(0) = H'(\lambda) = 0. (7.5)$$

By virtue of (2.3), any solution of (2.5), (2.7)-(2.9) gives a solution of (2.2), (7.3)-(7.5), and vice-versa.

In order to glean more information, we identify (7.3) with a dynamical system, treating "y" as a time-like variable. Then there are two critical points or "equilibria" corresponding to solutions of the algebraic equation

$$\dot{W}^*(H) - \varpi = 0. \tag{7.6}$$

The graph of \dot{W}^* reveals that there are precisely two solutions for $\dot{W}^*(\kappa) < \varpi \leqslant \gamma$, denoted $H \equiv \alpha$, and $H \equiv \beta$, where $0 \leqslant \alpha < \beta \leqslant M$. cf. Figure 3. In addition, (7.3) admits the first integral

$$\frac{\varepsilon}{2}(H')^2 - [W^*(H) - \varpi H] = \Gamma, \tag{7.7}$$

where Γ is a constant. With (7.7) in hand, we obtain the phase portraits depicted in Figure 5, where α is a "center", and β is a "saddle". According to the boundary conditions (7.5), the trajectories should "start and stop" on the H-axis. As such, we are interested only in closed orbits about the center

$$\alpha = 1/\lambda,\tag{7.8}$$

the value of which follows from (2.3), given that it represents the trivial solution $H \equiv 1/\lambda \iff u \equiv 0$. Moreover, we must chose only those orbits yielding even, periodic solutions having period $2\lambda/p, p = 1, 2, ...$ Recalling property (1.2)_, first integral (7.7) also implies that a nontrivial solution Hof(2.5), (2.7)-(2.9) with period $2\lambda/p$ has either a maximum at y = 0 and a minimum at $y = \lambda/p$, or vice-versa, with Hstrictly monotonic on $(0, \lambda/p)$,cf. [SG]. In view of (2.3), these same qualitative properties hold for nontrivial solutions of (3.3) or equivalently of (5.1). In fact it's worth stating the following:

Proposition 7.2 For any solution pair $(\lambda, u) \in \mathcal{C}_n \setminus \{(\lambda_n, 0)\}, n = 1, 2, ...,$ given by Theorem 5.1, it follows that u has minimal period 2/n, either u has a maximum at s = 0 and a minimum at s = 1/n or vice-versa, and u is strictly monotone on (0, 1/n).

Proof. Given the equivalence of systems (2.5), (2.7)-(2.9) and (2.2), (7.3)-(7.5) via (2.3), we see that u has period 2/p for some $p \in \mathbb{N}$, etc. So the only issue to address is the claim that p = n; this follows from (7.2). Indeed, if $p \neq n$, then (2.5) insures that u(0) and

u(1/p) have opposite signs. Thus, u has a single zero on (0, 1/p), leading to precisely p zeros on (0, 1). But this contradicts (7.2) unless p = n. \square

Remark 7.3 Referring again to (7.3), the cases $\varpi \leqslant \dot{W}^*(\kappa)$ and $\varpi > \gamma$ are not associated with solutions of (7.3), (7.5). The first leads to either one degenerate critical point $\alpha = \beta$ (for $\varpi \leqslant \dot{W}^*(\kappa)$) or no critical points, while the second case yields a critical point that violates (2.2)₂.

We now claim that "facture" occurs on each of the global solution branches, each of which is bounded.

Theorem 7.4 Each of the global bifurcating branches of Theorem 4.1, C_n , n = 1, 2, ..., is bounded in $\mathbb{R}^+ \times X^1$ and characterized solely by alternative (iii)' of Corollary 6.2.

Proof. In view of Proposition 7.1, if (i)' of Corollary 6.2 is not true then (iii)' is automatic. So it's enough to show that alternative (i)' does not hold. We argue by contradiction, assuming that (i)' is true. Then the bound (6.7) implies there is a sequence $\{(\lambda_j, u_j)\} \subset \mathcal{C}_n$ such that $\lambda_j \to \infty$. From (2.3) we obtain a sequence of solutions $\{(\lambda_j, H_j)\}$ of (2.2), (7.3)-(7.5), with

$$H_j(y) = [1 + u_j(y/\lambda_j)]/\lambda_j > 0 \text{ on } [0, \lambda_j],$$
 (7.9)

cf. (5.3). We also have a sequence of centers (7.8) satisfying

$$\alpha_j = 1/\lambda_j \searrow 0, \tag{7.10}$$

which implies that the phase portrait in Figure 5(b) is appropriate. With $\varpi_j := \dot{W}^*(\alpha_j)$, we also have the sequence of saddles for (7.3), coming from $\dot{W}^*(\beta_j) = \varpi_j$, satisfying $\beta_j \nearrow M$, viz., $\varpi_j \nearrow \gamma$, as $j \to \infty$,cf. Figure 3. Conditions (7.9) and (7.10) taken together imply that the amplitude of the "oscillation" about the center must also approach zero. That is, from (7.9), we have $0 < \delta_j := \min_{y \in [0,\lambda]} H^j(y) < \alpha_j = 1/\lambda_j$, and along that particular orbit, (7.7) yields

$$\frac{\varepsilon}{2}(H')^2 + \dot{W}^*(\alpha_j)H - W^*(H) = \Gamma_j, \tag{7.11}$$

where $\Gamma_j = \dot{W}^*(\alpha_j)\delta_j - W^*(\delta_j) \searrow 0$ as $j \to \infty$. But this contradicts the previously noted observation that the minimal period of the solution H_j is given by $T_j = 2\lambda_j/n \to \infty$ as $j \to \infty$. Indeed, referring to the phase portrait in Figure 5b, the period is an increasing function of Γ in (7.7) that approaches infinity as $\Gamma \nearrow \gamma$,cf. [A]. \square

We close this section with a strengthened version of Proposition 4.2, regarding the instability of the "higher-mode" global solution branches. For any solution pair $(\lambda, u) \in \mathcal{C}_n \setminus \{(\lambda_n, 0), \text{the second variation takes the form}$

$$\delta^2 V_{\varepsilon}[\lambda, u; \eta] := \frac{d^2}{d\tau^2} V_{\varepsilon}[\lambda, u + \tau \eta]|_{\tau=0} = \int_0^1 \left[\varepsilon(\eta')^2 + \lambda^2 \ddot{W}^*([1+u]/\lambda) \eta^2 \right] ds. \tag{7.12}$$

We observe that (7.12) is well defined for all $\eta \in \bar{H}^1(0,1)$, where $\bar{H}^1(0,1) := \{v \in H^1(0,1) : \int_0^1 v ds = 0\}$. We now use an argument form [CGS] to obtain the following instability result: **Proposition 7.5** For $(\lambda, u) \in \mathcal{C}_n \setminus \{(\lambda_n, 0), n = 2, 3, ..., the second variation (7.12) is strictly negative at some <math>\eta \in \bar{H}^1(0,1)$, i.e., u is unstable.

Proof. We first define

$$\varphi(s) := \left\{ \begin{array}{l} u'(s), \ 0 \leqslant s \leqslant 1/n, \\ 0, \ 1/n \ \leqslant s \leqslant 1, \end{array} \right.$$
 (7.13)

and choose any $\psi \in \bar{H}^1(0,1)$ such that

$$\psi(0) = 1 \text{ and } \psi(s) \equiv 0 \text{ for } 1/n \leqslant s \leqslant 1.$$
 (7.14)

By virtue of Proposition 7.2, it follows that

$$u'(1/n) = 0, (7.15)$$

and thus,

$$\eta_o := \phi + \tau \psi \in \bar{H}^1(0,1) \text{ for } \tau \in \mathbb{R}.$$

$$(7.16)$$

Substituting (7.16) into (7.12) yields

$$\delta^{2}V_{\varepsilon}[\lambda, u; \eta_{o}] = \int_{0}^{1/n} \left[\varepsilon(u'')^{2} + \lambda^{2} \ddot{W}^{*}([1+u]/\lambda)(u')^{2} \right] ds + 2\tau \int_{0}^{1/n} \left[\varepsilon u'' \psi' + \lambda^{2} \ddot{W}^{*}([1+u]/\lambda) u' \psi \right] ds + O(\tau).$$
(7.17)

From $(1.2)_{-}$, (2.7) and (2.8), we find that

$$\varepsilon u''' = \lambda^2 \ddot{W}^*([1+u]/\lambda)u'. \tag{7.18}$$

Substituting (7.18) into (7.17), while making use of (7.14), (7.15), leads to

$$\delta^2 V_{\varepsilon}[\lambda, u; \eta_o] = -2\tau u''(0) + O(\tau). \tag{7.19}$$

Finally, since u is a nontrivial solution, we know that $u''(0) \neq 0$. Otherwise, (2.3) would imply that H''(0) = 0, which contradicts (7.3) unless (7.6) is satisfied. Thus (7.19) is negative for sufficiently small τ . \square

Remark 7.6 Results for similar 1D models associated with phase transformations suggest that the first global branch should contain stable solutions for sufficiently small $\varepsilon > 0$, cf. [CGS], [LR]. We pursue this via a computational strategy in the next section.

8. Effective Macroscopic Behavior

In this section we interpret our results in terms of the conventional Lagrangian description, as discussed in Section 1. Taking the point of view of [LR], our goal is to obtain the effective or macroscopic stress-strain diagram based on the global solutions obtained and characterized in Sections 5-7. This is an alternative global bifurcation diagram. In view of Propositions 4.2 and 7.5, it's enough to consider only the trivial solution and the first global branch C_1 ; the latter is the only branch potentially containing stable solutions.

We first express (2.1), $(2.2)_1$ in terms of the deformation gradient

$$F(x) := f'(x) = 1/H(f(x)). \tag{8.1}$$

Recalling $y = f(x) \Leftrightarrow x = h(y)$, we likewise have

$$H(y) = h'(y) = 1/F(h(y)).$$
 (8.2)

By the chain rule and the change-of-variable formula, we find that

$$H'(f(x)) = -F'(x)/(F(x))^{3},$$
(8.3)

and the total energy becomes

$$\tilde{E}_{\varepsilon}[F] = \int_0^1 \left[\frac{\varepsilon}{2} \frac{(F')^2}{F^5} + W(F) \right] dx, \tag{8.4}$$

subject to

$$\int_0^1 F dx = \lambda. \tag{8.5}$$

The Euler-Lagrange equation for (8.4), (8.5) is readily obtained:

$$-\varepsilon \left[\left(\frac{F'}{F^5} \right)' + \frac{5}{2} \left(\frac{F'}{F^3} \right)^2 \right] + \dot{W}(F) = \sigma \text{ on } (0,1).$$
 (8.6)

where the multiplier σ , enforcing (8.5), represents the constant generalized stress carried by the bar. Indeed along the trivial, homogeneous solution $F \equiv \lambda$, we obtain the first-gradient constitutive law

$$\sigma = \dot{W}(\lambda),\tag{8.7}$$

which, in view of (1.3) and Figure 2a, is depicted in Figure _. Using (8.1)-(8.3) and the chain rule, it's not hard to see that (8.6) is equivalent to

$$\sigma = \varepsilon [H''H - \frac{1}{2}(H')^2] + W^*(H) - H\dot{W}^*(H) \text{ on } (0,\lambda), \tag{8.8}$$

where we have also employed (1.1). According to Theorem 7.4, the bounded solution branch C_1 contains a nontrivial solution $\operatorname{pair}(\lambda_*, u_*)\operatorname{with}\lambda_* \in \mathbb{R}^+$ and $u_*(s_o) = -1$ for some $s_o \in [0, 1]$,cf. Corollary 6.2. Moreover, by virtue of Proposition 7.2, u is strictly monotone, and thus either $s_o = 0$ or $s_o = 1$ (in fact, by symmetry both possibilities occur on C_1 , cf. Remark 3.2). In other words, the bar fractures at one of the two ends. We now show that the generalized stress vanishes at that solution, i.e., the fractured bar carries no stress.

Theorem 8.1 Suppose that $(\lambda_*, u_*) \in C_1$ is as described above. Then either $H_*(0) := (1 + u_*(0)/\lambda_* = 0 \text{ or } H_*(\lambda_*) := (1 + u_*(\lambda_*)/\lambda_* = 0, \text{ and the generalized stress (8.8) is identically zero at that solution.$

Proof. Without loss of generality, suppose that $u_*(0) = -1$. Then according to (2.3), $H_*(0) = 0$. From Proposition 7.2 and the discussion preceding it, we note that (8.8) is valid on \mathbb{R} mod 2. Evaluating (8.8) at y = 0 ($\Leftrightarrow s = 0$), while employing (1.2) and (7.5), we arrive at $\sigma = W^*(0) - 0 \cdot \gamma = 0$.

It is possible

According to Proposition 3.1 and Theorem 7.4, the bounded solution branch C_1 connects the bifurcation point $(\lambda_1, 0)$ to the "fracture" point (λ_*, u_*) , described above. In terms of the stress-strain diagram of Figure_, the bifurcation point is located at $(\lambda_1, \dot{W}(\lambda_1))$, where $\lambda_1 > 1/\kappa$, cf. (2.13). Moreover, in view of Theorem 8.1, the fracture point is located at $(\lambda_*, 0)$, for $\lambda_* \in \mathbb{R}^+$. With λ now playing the role of macroscopic strain, viz., $\lambda = f(1)$, the projection of C_1 onto the σ vs. λ plane connects $(\lambda_1, \dot{W}(\lambda_1))$ to $(\lambda_*, 0)$.

In order to compute the first global branch we turn to the methodology of Carr, Gurtin & Slemrod[?]. For $0 \le a < b < 1$ and $z \ge 0$, let

$$U(z,a,b) = W^*(z) - \varpi(a,b)z + \Gamma(a,b), \tag{8.9}$$

where

$$\varpi(a,b) = \frac{W^*(b) - W^*(a)}{b - a}, \qquad \Gamma(a,b) = \varpi(a,b)a - W^*(a),$$
(8.10)

and (formally) define

$$g_0(a,b) = \int_a^b \frac{1}{\sqrt{U(z,a,b)}} dz, \quad g_1(a,b) = \int_a^b \frac{z}{\sqrt{U(z,a,b)}} dz$$
 (8.11)

Proposition 8.2. (i) Suppose $(\lambda, u) \in C_1$ with H(y) as in (2.3). Let $H(0) = H_2$ and $H(\lambda) = H_1$. Then these satisfy

$$0 \le H_1 < \kappa, \quad H_1 < H_2 < 1, \quad U(H, H_1, H_2) > 0 \quad \forall H \in (H_1, H_2)$$
 (8.12)

$$\sqrt{\frac{\varepsilon}{2}}g_0(H_1, H_2) = \lambda, \qquad \sqrt{\frac{\varepsilon}{2}}g_1(H_1, H_2) = 1$$
(8.13)

Moreover the generalized stress σ from (8.6) is given by

$$\sigma = W^*(H_1) - \varpi(H_1, H_2)H_1 \tag{8.14}$$

(ii) For each $H_1 \in [0, 1/\lambda_1)$, the second of (8.13) is uniquely solvable for $H_2 = \hat{H}(H_1)$. Define

$$\hat{\lambda}(H_1, \varepsilon) = \sqrt{\frac{\varepsilon}{2}} g_0(H_1, \hat{H}(H_1)), \quad \hat{\sigma}(H_1) = W^*(H_1) - \varpi(H_1, \hat{H}(H_1))H_1$$
 (8.15)

Then the above is a parametrization of the image of C_1 onto the (λ, σ) plane.

(iii) Setting $H_1 = 0$ above gives the fracture point $(\lambda, \sigma) = (\lambda_*, 0)$ where C_1 contacts the zero-stress line. More specifically,

$$1 < \lambda_* = \hat{\lambda}(0, \varepsilon) \searrow 1$$
 as $\varepsilon \searrow 0$.

Remark. Given an inverse strain profile H from the 1st branch C_1 , this result allows us to determine the point (λ, σ) on the effective or macroscopic stress-strain diagram. Typically we (numerically) solve the second of (8.13) for H_2 in terms of H_1 . This gives the parametrization (8.15) of (λ, σ) .

Proof of Proposition 8.2.(i) By hypothesis, Proposition 7.2 with n=1 and the phase portrait (see discussion leading to (7.8)) H is strictly monotone on $[0,\lambda]$ and $H'(y) \neq 0$ except at $y=0, \lambda$, thus (7.7) and the natural boundary conditions (7.5), imply that $W^*(H) - \varpi H + \Gamma > 0$ for $H \in (H_1, H_2)$ and vanishes for $H = H_i$, i=1,2. This in turn shows that

$$W^*(H) - \varpi H + \Gamma = U(H, H_1, H_2)$$
(8.16)

and that the third inequality in (8.12) holds, which implies the first two. Substituting (8.16) in (7.7), solving for H' and keeping the negative of the two solutions (the other giving equivalent results) we infer

$$H'(y) = -\sqrt{(2/\varepsilon)U(H(y), H_1, H_2)}, \quad y \in [0, \lambda]$$
 (8.17)

This can be solved for the inverse $y = \hat{y}(H)$ of H(y), noting that $\hat{y}(H_1) = 0$, yielding

$$\hat{y}(H) = \sqrt{\frac{\varepsilon}{2}} \int_{H_1}^{H} \frac{1}{\sqrt{U(z, H_1, H_2)}} dz$$

The requirement that $\hat{y}(H_2) = \lambda$ then gives the first of (8.13), while the integral constraint (2.2) reduces to the second of (8.13) after changing variables from y to H. Next, use (7.3) and (7.7) to eliminate H'' and H', respectively, from (8.8), deducing that $\sigma = -\Gamma$. This confirms (8.14) in view of (8.10), in view of (8.16).

Proposition 8.3. Let $H_*: [0, \lambda_*] \to [0, 1]$ be the inverse strain solution at the fracture point $(\lambda_*, 0)$. For $\lambda > \lambda_*$ define

$$H_b(y) = \begin{cases} H_*(y), & 0 \le y \le \lambda_*, \\ 0, & \lambda_* < y \le \lambda. \end{cases}$$
 (8.18)

Then H_b is a broken solution (with zero stress $\sigma=0$) of the Euler-Lagrange inequality corresponding to (2.1). In addition, as $\varepsilon \to 0$, the energy (2.1) is

$$E_{\varepsilon}[H_b] = \sqrt{\varepsilon} \int_0^1 \sqrt{2W^*(H)} dH + o(\sqrt{\varepsilon}) = \sqrt{\varepsilon} \int_1^\infty \sqrt{2W(F)/F^5} dF + o(\sqrt{\varepsilon})$$
 (8.19)

Remark. After the bar breaks at λ_* , we can continue pulling the broken end $y = \lambda_*$ further to any $\lambda > \lambda_*$. The interval $\lambda_* < y < \lambda$ is "aether" or vacuum H = 0 or " $F = \infty$ " namely a displacement discontinuity, the famous crack-opening displacement. Here there is a transition layer from H close to 1 to H = 0 of size approximately $\sqrt{\varepsilon}$. Morevover the first formula in (8.19) is formally identical to the interfacial energy of a phase boundary with higher gradients [?], so this energy can be interpreted as the surface energy of fracture in ther sense of Griffith [].

Proof of Proposition 8.3. The Euler-Lagrange inequality becomes

$$-\varepsilon H''(y) + \dot{W}^*(H(y)) \begin{cases} = \varpi, & y \in \mathcal{G} = \{ y \in [0, \lambda] : H(y) > 0 \}, \\ \geq \varpi, & y \in \mathcal{B} = \{ y \in [0, \lambda] : H(y) = 0 \}. \end{cases}$$
(8.20)

cf. (7.5), together with the natural boundary conditions and smoothness requirements

$$H' = 0$$
 on $\partial \mathcal{G}$, $H \in C^1([0, \lambda])$, $H = 0$ on $\partial \mathcal{B}$

Choosing $H = H_b$ from (8.18) we identify the "glued" set $\mathcal{G} = [0, \lambda_*)$ and the "broken" or coincidence set $\mathcal{B} = [\lambda_*, \lambda]$. Now H_* satisfies (8.17) with $H_1 = 0$ (for $y \in [0, \lambda_*]$) so squaring and differentiating it shows that the first case in (8.20) holds. Upon setting H(y) = 0 in the second case, and noting that $\dot{W}^*(0) = \gamma$ we obtain $\varpi \leq \gamma$, which holds true, since by

(8.10), $\varpi = \varpi(0, H_2)$ equals the slope of a chord joining two points on the strictly concave graph of W^* , whose maximum slope at H = 0 is γ .

Next, write the energy of H_b as follows, observing the constraint $\int_0^{\lambda} H(y)dy = 1$, that $H_b = 0$ on $[\lambda_*, \lambda]$ by (8.18), that $W^*(0) = 0$ and using .

$$E_{\varepsilon}[H_{b}] = \int_{0}^{\lambda} \left(\frac{\varepsilon}{2} [H'_{b}(y)]^{2} + W^{*}(H_{b}(y)) - \varpi[H_{b}(y) - 1/\lambda]\right) dy$$

$$= \int_{0}^{\lambda_{*}} \left(\frac{\varepsilon}{2} [H'_{b}(y)]^{2} + W^{*}(H_{*}(y)) - \varpi H_{*}(y)\right) dy + \varpi$$

$$= \int_{0}^{\lambda_{*}} \left(\frac{\varepsilon}{2} [H'_{b}(y)]^{2} + U(H_{*}(y), 0, H_{2}(\varepsilon))\right) dy + \varpi(0, H_{2}(\varepsilon))$$

$$= \int_{0}^{\lambda_{*}} 2U(H_{*}(y), 0, H_{2}(\varepsilon) dy + \varpi(0, H_{2}(\varepsilon))$$

$$= \sqrt{\varepsilon} \int_{0}^{H_{2}(\varepsilon)} \sqrt{2U(H_{*}(0), H_{2}(\varepsilon))} dH + \varpi(0, H_{2}(\varepsilon))$$

where we have used (8.17) to obtain the fourth line above and the change of variables for the fifth line. Here $H_2(\varepsilon)$ is the root of the second of (8.13) with $H_1 = 0$. As shown by CGS [?]...

In order to gain more information concerning the location of λ_* , and to infer stability properties, we turn to a specific model and compute the first global branch of solutions. Specifically, we choose $W^*(H) = H(1-H)^2$, which follows from $W(F) = (1-1/F)^2$ via (1.1).

We introduce a special W^* that is piecewise-quadratic, so that the Euler-Lagrange equation is (piecewise) linear. Let

$$\kappa = 1/\sqrt{2}, \quad d = \sqrt{2} - 1$$

and define

$$W^*(H) = \begin{cases} d^2 - (H - d)^2, & 0 \le H \le \kappa, \\ (H - 1)^2, & \kappa < H < \infty. \end{cases}$$
 (8.21)

Suppose we look at solutions of (2.7) such that $0 < H(x) < \kappa$ for $0 < x < \lambda$, so that

$$-1 < u(s) < \kappa \lambda - 1, \quad s \in (0, 1)$$
 (8.22)

in (2.7) (this demands that $\lambda > 1/\kappa$). Then (2.7) becomes linear and reduces exactly to (2.10), whose solutions are $u(s) = A\cos(n\pi s)$, $0 \le s \le 1$, for some constant A, with λ restricted to satisfy (2.12) namely $\lambda = \lambda_n = n\pi\sqrt{\varepsilon/2}$. The bifurcation condition thus holds all along each branch, from A = 0 at bifurcation, all the way to fracture where |A| = 1, so that u = -1 at one end. The second inequality in (8.22) then asserts $\kappa\lambda \ge 2$ namely $\varepsilon > 16/\pi^2$. Branches in the (λ, σ) plane are vertical lines form the trivial branch (stress-stretch curve $\sigma = 1/\lambda^2$, all the way down to $\sigma = 0$ with $\lambda = \lambda_n = n\pi\sqrt{\varepsilon/2}$.

REMARK: For $\varepsilon < 16/\pi^2$ part of the branch near the bottom involves solutions u that violate (8.22) in part of the domain. These are trigonometric in part of the domain and exponential in the rest. These can be computed more or less explicitly modulo solution of nonlinear algebraic equation for the parameters. but the simple ones are the purely trigonometric ones where the 2nd variation can be computed explicitly. Can we investigate the stability of these?

SOLUTIONS FOR $\varepsilon > 16/\pi^2$:

$$u(s) = A\cos(n\pi s), \quad 0 \le A \le 1, \qquad \lambda = \lambda_n = n\pi\sqrt{\varepsilon/2}$$

References

[Kiel] H. Kielhöfer, Bifurcation Theory, 2nd Ed., Springer 2012

[CR] Crandall and Rabinowitz, Bifurcation from simple eigenvalues, J. Functional Anal. 8 (1971) 321-340.

[R] Rabinowitz, Some global results for nonlinear eigenvalue problems, J. Functional Anal. 7 (1971) 487-513.

[CR2] Crandall and Rabinowitz, Nonlinear Sturm-Liouville eigenvalue problems and topological degree, J. Math. Mech. 19 (1970) 1083-1102.

[SG] Synge and Griffith, Principles of Mechanics, McGraw-Hill 1959. [Shield]

[Carlson and Shield]

[A] V.I. Arnold, Mathematical Methods of Classical Mechanics, Springer